Synthesis, Structure Determination, and Magnetic Properties of $[Cr_3(dpa)_4Cl_2][CuCl_2]$, a Compound Comprising a Trinuclear Chain Cation

Dilahan Aydin-Cantürk and Hanne Nuss

Max-Planck-Institut für Festkörperforschung, Heisenbergstraße 1, 70569 Stuttgart, Germany

Reprint requests to H. Nuss. Fax: +49-711-689-1502. E-mail: h.nuss@fkf.mpg.de

Z. Naturforsch. **2012**, *67b*, 759 – 764 / DOI: 10.5560/ZNB.2012-0163
Received June 14, 2012

The new compound $[Cr_3(dpa)_4Cl_2][CuCl_2]$ (**1**) (dpa = di-2,2′-pyridylamido) was synthesized by reacting $Cr_2(dpa)_4$ and anhydrous $CuCl_2$ in dry tetrahydrofuran. Partial oxidation of $Cr_2(dpa)_4$ by Cu(II) forms Cr^{3+} ions, which coordinate to the free N donor atoms of the dpa ligands, and led to the formation of a trinuclear chain cation $[Cr_3(dpa)_4Cl_2]^+$. Recrystallization from CH_2Cl_2/ethyl ether yielded dark-brown, block-shaped crystals suitable for X-ray structure determination (*Pccn* (no. 56), $a = 1246.8(5)$, $b = 1487.3(3)$, $c = 2184.8(1)$ pm, $V = 4051.6(8) \cdot 10^6$ pm^3, $Z = 4$). The crystal structure is composed of discrete $[Cr_3(dpa)_4Cl_2]^+$ cations and $[CuCl_2]^-$ anions. The Cr_3 chain comprises quadruply-bonded diamagnetic $(Cr_2)^{4+}$ dimers and a pseudo-octahedrally coordinated, paramagnetic Cr^{3+} ion, manifesting itself in the effective magnetic moment μ_{eff} of $3.54\mu_B$ (d^3, $S = 3/2$) and the almost ideal Curie-paramagnetic behavior observed between 2 and 300 K with a Weiss constant $\theta = -0.25(4)$ K and $\chi_0 = 4.9(7) \times 10^{-4}$ emu mol^{-1}.

Key words: Trinuclear Chromium Complexes, Dichlorocuprate(I) Anion, Extended Metal Atom Chains, Magnetic Properties, Multiple Bonds, Mixed Valence

Introduction

In terms of "molecular wire-like materials", extended metal atom chains (EMACs) of the type $M_n(L)_4X_2$ (M = transition metal, L = equatorial ligands *e. g.* polypyridylamide, and X = axial ligands, *e. g.* halide or pseudo-halide ions) get more and more attention [1, 2]. Besides the synthesis of longer metallic chains, supported by appropriate organic ligands [3], the formation of heterometallic chain compounds is investigated in order to get a deeper insight into the metal-metal interactions within the chain, and the influences of the chemical environment on it, respectively [4]. Chromium-based EMACs, as introduced by Cotton *et al.*, have drawn the attention due to multiple bond formation of Cr and the resulting variability in metal-metal interactions and metal oxidations states of the terminal chromium atoms [5 – 11]. Recently, Berry *et al.* were able to substitute terminal metal atoms of three-membered chains comprising Cr, Mo, or W atoms in a controlled manner and presented the first heterometallic chain compounds within this family. They observed a significant influence of the $(Cr_2)^{4+}$ dimer on the terminal heterometal (*e. g.* Fe, Mn, Co) manifesting itself, for example, in the ease of its oxidation [12 – 16].

In this work we present the new EMAC $[Cr_3(dpa)_4Cl_2][CuCl_2]$ (dpa = di-2,2′-pyridylamido) as an oxidation product of the precursor $Cr_2(dpa)_4$ with $CuCl_2$. Instead of simply incorporating Cu^{2+} into the chain, a redox reaction leads to the formation of a mixed-valent $[Cr^{II}Cr^{II}Cr^{III}(dpa)_4Cl_2]^+$ cation and the linear $[CuCl_2]^-$ anion.

Results and Discussion

Synthesis

The general synthesis route to heterometallic chain compounds, as introduced by Berry *et al.*, involves the generation of a quadruply-bonded precursor $M_2(dpa)_4$ with M = Cr(II), Mo(II) or W(II) and dpa = 2,2′-dipyridylamide and its reaction with a divalent metal

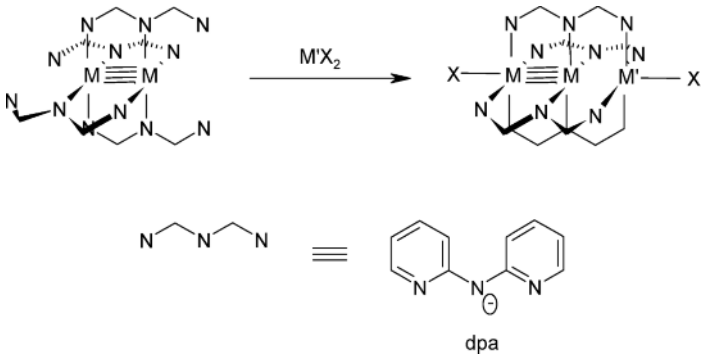

Scheme 1.

salt MX_2 (M = Mn(II), Fe(II), Co(II), Ni(II) or Zn(II); X = *e. g.* halide) as shown in Scheme 1 [12 – 16].

However, the reaction of $Cr_2(dpa)_4$ with $CuCl_2$ in tetrahydrofuran does not lead to the expected CrCrCu chain, but yields the title compound *via* a redox reaction and incorporation of the *in situ*-produced Cr^{3+} ions. The obtained $[Cr_3(dpa)_4Cl_2]^+$ complex cation is already known and was synthesized by Cotton *et al.* *via* intentional oxidation of several $Cr_3(dpa)_4X_2$-type compounds (X = *e. g.* Cl^-, BF_4^-) [7]. The direct oxidation of a part of the $Cr_2(dpa)_4$ precursor by a divalent metal salt, has, to the best of our knowledge, not yet been observed.

Structure description

$[Cr_3(dpa)_4Cl_2][CuCl_2]$ (**1**) crystallizes as dark-brown, block-shaped crystals in the space group *Pccn* (no. 56) with 4 formula units per unit cell (Table 1, Figs. 1 and 2). The structure comprises linear dichlorocuprate(I) anions, $[CuCl_2]^-$, and $[Cr_3(dpa)_4Cl_2]^+$ complex cations. A projection of the crystal structure onto (001) (Fig. 1a) shows that the cation packing leads to the formation of channels, occupied by linear dichlorocuprate(I) anions. Since the axis of the anion lies on a two-fold axis, only the Cu–Cl bond lengths are refineable parameters, yielding values of 210.7(1) and 211.4(1) pm. Comparison with literature data shows that these values fit perfectly to Cu–Cl bond lengths of anions with a symmetry constraint to the Cl–Cu–Cl angle, where d(Cu–Cl) > 210 pm are observed [17]. Dichlorocuprate(I) anions with no angle constraint usually show, besides Cl–Cu–Cl angles < 180° (175° < ∠(ClCuCl) < 180°), slightly shorter bonds with 206 ≤ d ≤ 210 pm [18 – 22].

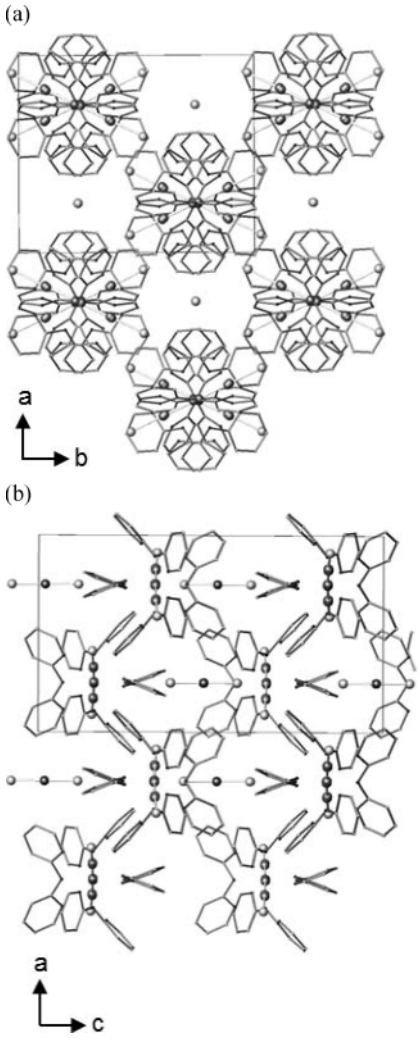

Fig. 1. Cut-out of the crystal structure of **1** projected on a) (001) and b) (010). Hydrogen atoms are omitted for clarity.

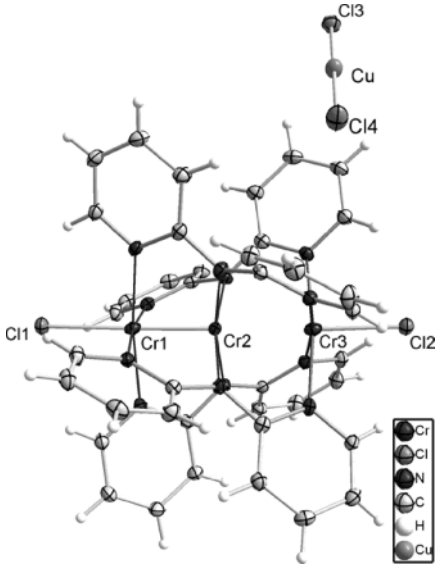

Fig. 2. Molecular structure of **1** (only one orientation of the disordered metal atoms is shown). Displacement ellipsoids are drawn at the 50 % probability level.

The Cr_3 chain in $[Cr_3(dpa)_4Cl_2]^+$ is built of a quadruply-bonded $(Cr_2)^{4+}$ dimer and an appended Cr^{3+} ion, stabilized by the coordination of four chelating 2,2′-dipyridylamide ligands. As often found in this family of compounds, an intrinsic orientational disorder of the chain is observed. Attempts to resolve this disorder by symmetry reduction – refinements in the maximal *translationengleiche* subgroups $Pna2_1$ (no. 33) and $P2_1/c$ (no. 14) being performed – remained unsuccessful. Nevertheless, the site occupation factors (sof) of the chromium positions for the two possible orientations (Cr1–Cr2···Cr3 and Cr1···Cr2–Cr3, where "–" indicates the short quadruple bond) converged in all low-symmetry refinements to about 50 % (49 : 51). The split position of the center chromium atom Cr2 can be resolved, whereas the difference in the terminal Cr position is too small.

For the final model, therefore, a description using the higher-symmetry space group *Pccn* has been chosen with all Cr positions refined with fixed sof's of 0.5, and all but the terminal chromium atoms and the hydrogen atoms, of course, have been refined anisotropically, in order to get the most reliable bond lengths (Table 2). The Cr–Cr distances in the dimer $(Cr_2)^{4+}$ of 201.8(2) pm and the contact of $(Cr_2)^{4+}$ to Cr^{3+} of 253.6(2) pm lie perfectly in the range of contacts of similar compounds reported by Clérac *et al.* [7]. The distances of Cr(II) and Cr(III) to the axial chlorine ligands can be distinguished and amount to 240.5(2) (Cr(II)–Cl) and 226.3(2) pm (Cr(III)–Cl), respectively.

Table 1. Crystal structure data for **1**.

Compound	$[Cr_3(dpa)_4Cl_2][CuCl_2]$
Formula	$C_{40}H_{32}N_{12}Cl_4Cr_3Cu$
Crystal system	orthorhombic
M_r	1042.12
Crystal size, mm^3	$0.12 \times 0.08 \times 0.08$
Space group (no.)	*Pccn* (56)
a, pm	1246.85(7)
b, pm	1487.33(8)
c, pm	2184.8(1)
V, $\times 10^6$ pm^3	4051.7(4)
T, K	100(2)
Z	4
D_{calcd}, $g\,cm^{-3}$	1.71
F(000), e	2100
μ, mm^{-1}	1.6
hkl range	±19, ±23, ±34
2θ range, deg	3.72 – 69.78
Refl. measured/unique/R_{int}	59 579/8560/0.0649
Ref. parameters	340
R_1 $[F^2 > 4\sigma(F^2)]/wR_2$ (all data)	0.0881/0.1336
GoF (F^2)	1.149
$\Delta\rho_{fin}$ (max/min), e $Å^{-3}$	0.86/ – 0.69

Table 2. Selected bond lengths (pm) and angles (deg) for **1** with estimated standard deviations in parentheses; $\langle x \rangle$ indicates mean value; symmetry code: (i) $-x+3/2, -y+1/2, z$.

Distances	
Cr1′–Cr2	253.6(2)
Cr2–Cr3	201.8(2)
Cr3–Cl	240.5(2)
Cr1′–Cl1	226.3(2)
⟨Cr1–N⟩	210.5
⟨Cr2–N⟩	199.3
⟨Cr3–N⟩	209.6
Cu1-Cl2	211.4(1)
Cu1-Cl3	210.7(1)
Angles	
Cr1–Cr2–Cr3′	176.9(1)
Cr2–Cr1–Cl1	178.0(1)
Cr2–Cr3–Cl1	178.6(1)
Cl2–Cu1–Cl3	180

Vibrational spectroscopy

Raman and IR spectra of **1** are shown in Figs. 3 and 4, respectively. The bands in the region 600 – 1600 cm^{-1}, which is dominated by vibration modes of the dpa ligand, agree very well with the results of a sophisticated vibrational analysis of sim-

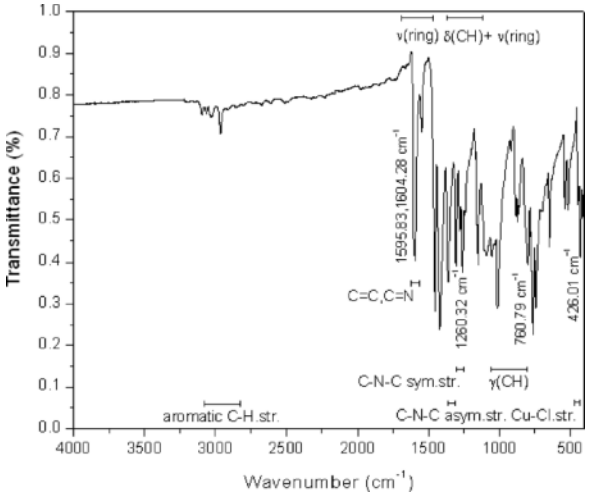

Fig. 3. IR spectrum of **1**.

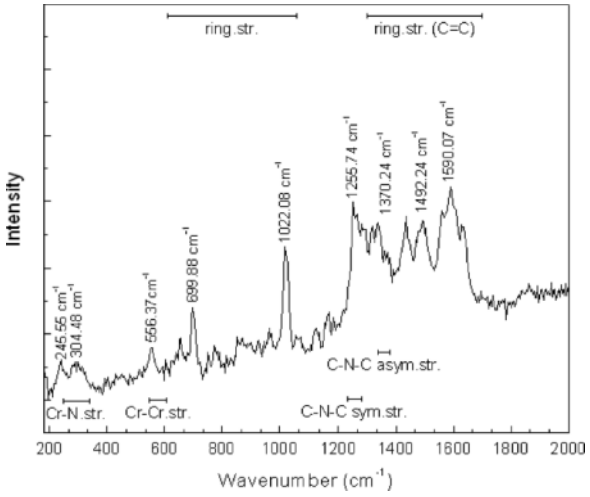

Fig. 4. Raman spectrum (180–2000 cm^{-1}) of **1**.

ilar compounds, $Cr_3(dpa)_4Cl_2$, $Cr_3(dpa)_4(NCS)_2$ and $[Cr_3(dpa)_4Cl_2](PF_6)$, as performed by Peng *et al.* [23]. The Raman line at 556 cm^{-1} indicates the stretching mode of the Cr_2 quadruple bond (IR inactive). The $[CuCl_2]^-$ anion gives rise to two characteristic signals, the IR-active asymmetric Cl–Cu–Cl stretching mode at 426 cm^{-1} and the symmetrical stretching mode observed in the Raman spectrum at 304 cm^{-1} [24].

Magnetic properties

The magnetic susceptibility of **1** was measured between 2 to 300 K. Fig. 5 shows the temperature dependence of the magnetic response of a powder sample at 0.1 T. A simple paramagnetic behavior is observed, with a μ_{eff} of 3.54 μ_B and a small negative Weiss constant θ of $-0.25(4)$ K, which indicates almost ideal Curie behavior. The magnetic moment of 3.54 μ_B is comparable to those found for other $[Cr_3(dpa)_4Cl_2]^+$-containing compounds, such as $[Cr_3(dpa)_4Cl_2]Cl{\cdot}2CH_2Cl_2{\cdot}THF$ ($\mu_{eff} = 3.9\mu_B$) and $[Cr_3(dpa)_4Cl_2]AlCl_4{\cdot}CH_2Cl_2$ ($\mu_{eff} = 3.8\mu_B$) [7] and supports the structural description of the Cr_3 chain as being composed of a diamagnetic quadruply bonded pair of Cr^{2+} cations and a paramagnetic Cr^{3+} cation. The effective moment found fits to values usually observed for octahedrally coordinated Cr^{3+} cations (d^3, $S = 3/2$) with 3 unpaired electrons.

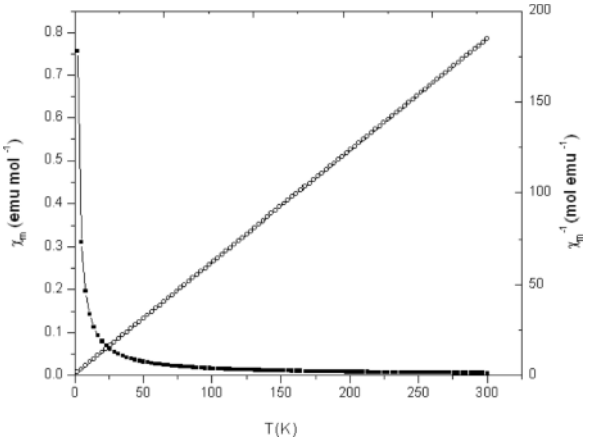

Fig. 5. Temperature dependence of the magnetic susceptibility (■) und its inverse (○) at 0.1 Tesla.

Conclusion

The synthesis of $[Cr_3(dpa)_4Cl_2][CuCl_2]$ from $Cr_2(dpa)_4$ *via* direct oxidation with $CuCl_2$ presents an alternative way to the formation of the extended metal atom chain in $[Cr_3(dpa)_4Cl_2]^+$. The two possible orientations of the disordered homonuclear metal chain emerge in equal parts, and the disorder cannot be resolved by symmetry reduction even on low temperature data (100 K). Vibrational spectroscopy and magnetic measurements clearly support the structural description of the homonuclear Cr_3 chain, as being built of a quadruply-bonded diamagnetic $(Cr_2)^{4+}$ dimer, to which a paramagnetic, pseudo-octahedrally coordinated Cr^{3+} unit is attached. The geometry observed for

the dichlorocuprate(I) anion fits very well to values reported for other symmetry-constrained $[CuCl_2]^-$ ions.

Experimental Section

Materials and measurements

All manipulations were performed under an argon atmosphere using standard Schlenk techniques or in a glove box. Solvents were dried according to standard procedures and freshly distilled prior to use. Anhydrous $CrCl_2$ and $CuCl_2$ (99.9 %, both Alfa Aesar), di-2,2′-pyridylamine (99 %, Sigma-Aldrich) and methyllithium (Acros Organics, 1.6 M in Et_2O) were used as received. $Cr_2(dpa)_4$ was synthesized according to the procedure described by Cotton *et al*. [25]. Magnetic susceptibilities were determined with a SQUID magnetometer (MPMS7 Quantum Design, USA) in applied fields of 0.1, 1, and 7 T over the temperature range 2 – 300 K. Powder samples were sealed into Suprasil quartz tubes filled with helium gas enabling fast thermal equilibration. Data were corrected for the diamagnetic contributions of the sample, using the increment method of Pascal, Gallais, and Labarre [26]. Infrared spectra of KBr pellets were taken with a FT-IR spectrometer (Bruker IFS 113v) at ambient temperature in an evacuated sample chamber. Raman spectra of samples sealed in Suprasil quartz glass ampoules were recorded at r. t. with a Jobin Yvon Typ V 010 labram single grating spectrometer with a resolution of 3 cm^{-1}, equipped with a double super razor edge filter and a Peltier cooled CCD camera. The spectra were taken in quasi-backscattering geometry using the linearly polarized 532.0 nm line of a diode laser with power less than 1.0 mW, focused to a 15 μm spot through a 20× microscope objective on to the top surface of the sample.

Synthesis

In a Schlenk flask, equipped with a reflux condenser, a mixture of $Cr_2(dpa)_4$ (100 mg, 0.12 mmol) and $CuCl_2$ (25 mg, 0.18 mmol) in tetrahydrofuran (12 mL) was heated to reflux for 7 h. After stirring for 5 days at room temperature the dark-brown reaction mixture was filtered, and the solvent was removed *in vacuo* yielding a greenish-brown solid. Recrystallization of the solid from CH_2Cl_2-Et_2O (6 mL) gave after 24 h dark-brown block-shaped crystals, suitable for X-ray crystal structure determination (23.8 mg, 15 %). EDX (energy dispersive X-ray analysis): ratio Cl : Cr : Cu = 4 : 3 : 1. – IR (KBr): ν = 3095.68 (m), 3064.51 (m), 3027.74 (m), 2963.00 (m), 1604.28 (s), 1596.83 (s), 1547.74 (m), 1454.43 (s), 1422.37 (s), 1363.47 (s), 1306.50 (m), 1279.84 (m), 1260.32 (m), 1242.21 (w), 1170.25 (vw), 1149.50 (m), 1104.58 (m), 1048.79 (w), 1014.64 (m), 917.89 (w), 881.86 (m), 869.67 (m), 798.22 (m), 760.79 (s), 741.77 (s), 645.94 (m), 537.90 (m), 515.21 (m), 443.12 (m), 426.01 (s) cm^{-1}.

X-Ray structure determination

For single-crystal structure determination, suitable crystals were selected under high viscous inert oil, attached to the tip of a kapton loop (MicroMounts™, MiTeGen, Ithaca/USA) and mounted on a pre-cooled goniometer head (cold, dry N_2 gas stream).

Intensity data were collected at 100(2) K with a Smart APEX II diffractometer (Bruker AXS, Karlsruhe, Germany) with MoK_α radiation (λ = 0.71073 Å) and a graphite monochromator. A semi-empirical absorption correction was applied using SADABS [27]. The structure was solved with Direct Methods and refined using the program package SHELXTL [28]. Crystallographic data and structure refinement results are summarized in Table 1, selected bond lengths and angles are given in Table 2.

CCDC 884822 contains the supplementary crystallographic data for this paper. These data can be obtained free of charge from The Cambridge Crystallographic Data Centre *via* www.ccdc.cam.ac.uk/data_request/cif.

Acknowledgement

We would like to thank Mr. A. Schulz for collecting the Raman spectra and Mrs. E. Brücher for conducting the SQUID measurements. H. N. also thanks Prof. Dr. Dr. h. c. M. Jansen for support.

[1] J. F. Berry, *Struct. Bond.* **2010**, *136*, 1 – 28.
[2] J. K. Bera, K. R. Dunbar, *Angew. Chem. Int. Ed.* **2002**, *23*, 4453 – 4457.
[3] R. H. Ismayilov, W.-Z. Wang, G.-H. Lee, C.-Y. Yeh, S.-A. Hua, Y. Song, M.-M. Rohmer, M. Bérnard, S.-M. Peng, *Angew. Chem. Int. Ed.* **2011**, *50*, 2045 – 2048.
[4] M. Nippe, J. Wang, E. Bill, H. Hope, N. S. Dalal, J. F. Berry, *J. Am. Chem. Soc.* **2010**, *132*, 14261 – 14272.
[5] J. F. Berry, F. A. Cotton, T. Lu, C. A. Murillo, B. K. Roberts, X. Wang, *J. Am. Chem. Soc.* **2004**, *126*, 7082 – 7096.
[6] S.-Y. Lin, I.-W. Peter Chen, C.-H. Chen, M.-H. Hsieh, C.-Y. Yeh, T.-W. Lin, Y.-H. Chen, S.-M. Peng, *J. Phys. Chem. B* **2004**, *108*, 959 – 964.
[7] R. Clérac, F. A. Cotton, L. M. Daniels, K. R. Dunbar, C. A. Murillo, I. Pascual, *Inorg. Chem.* **2000**, *39*, 752 – 756.

[8] R. Clérac, F. A. Cotton, L. M. Daniels, K. R. Dunbar, C. A. Murillo, I. Pascual, *Inorg. Chem.* **2000**, *39*, 748 – 751.
[9] F. A. Cotton, L. M. Daniels, C. A. Murillo, I. Pascual, *Inorg. Chem. Commun.* **1998**, *1*, 1 – 3.
[10] T.-W. Tsai, Q.-R. Huang, S.-M. Peng, B.-Y. Jin, *J. Phys. Chem. C* **2010**, *114*, 3641 – 3644.
[11] F. A. Cotton, L. M. Daniels, C. A. Murillo, I. Pascual, *J. Am. Chem. Soc.* **1997**, *119*, 10223 – 10224.
[12] M. Nippe, J. F. Berry, *J. Am. Chem. Soc.* **2007**, *129*, 12684 – 12685.
[13] M. Nippe, E. Victor, J. F. Berry, *Eur. J. Inorg. Chem.* **2008**, 5569 – 5572.
[14] M. Nippe, E. Bill, J. F. Berry, *Inorg. Chem.* **2011**, *50*, 7650 – 7661.
[15] M. Nippe, Y. Turov, J. F. Berry, *Inorg. Chem.* **2011**, *50*, 10592 – 10599.
[16] D. Aydin-Cantürk, H. Nuss, *Z. Anorg. Allg. Chem.* **2011**, *637*, 543 – 546.
[17] H.-X. Guo, Z.-M. Rao, Q.-H. Wang, *Acta Crystallogr.* **2007**, *E63*, m637 – m638.
[18] P. C. Healy, J. C. McMurtrie, J. Bouzaid, *Acta Crystallogr.* **2010**, *E66*, 493 – 494.
[19] J.-G. Wang, H.-X. Kang, X.-Y. Zheng, *Z. Kristallogr.* **2005**, *220*, 597 – 598.
[20] Q. Meng, Y. Chen, B. Li, S. Chen, S. Gao, *Acta Crystallogr.* **2011**, *E67*, 226.
[21] H.-F. Yang, C.-C. Huang, H.-H. Zhang, Y. Liu, Z.-X. Lian, G.-C. Xiao, *Acta Crystallogr.* **2004**, *E60*, 291 – 293.
[22] G. Newton, H. D. Caughman, R. C. Taylor, *J. Chem. Soc., Dalton Trans.* **1974**, *3*, 258 – 264.
[23] C.-J. Hsiao, S.-H. Lai, I.-C. Chen, W.-Z. Wang, S.-M. Peng, *J. Phys. Chem. A* **2008**, *112*, 13528 – 13534.
[24] J. Weidlein, U. Müller, K. Dehnicke, *Schwingungsfrequenzen II*, Georg Thieme Verlag, Stuttgart **1986**, p. 36.
[25] F. A. Cotton, L. M. Daniels, C. A. Murillo, I. Pascual, H.-C. Zhou, *J. Am. Chem. Soc.* **1999**, *121*, 6856 – 6861.
[26] R. R. Gupta in *Landolt-Börnstein*: *Numerical Data and Functional Relationships in Science and Technology, New Series* (Eds.: K.-H. Hellwege, A. M. Hellwege), Vol. 16, Springer, Berlin, Germany **1986**, pp. 1 – 10.
[27] G. M. Sheldrick, SADABS (version 2007/4), Area Detector Scaling and Absorption, University of Göttingen, Göttingen (Germany) and Bruker Analytical X-ray Instruments Inc., Madison, Wisconsin (USA) **2007**.
[28] G. M. Sheldrick, *Acta Crystallogr.* **2008**, A64, *112*–122.